Supplementary information

Materials and Methods

Enrichment analysis

Gene Ontology (GO) and REACTOME enrichment analyses were performed using the HypeR function (hypeR and msigdbr libraries) in R (see R code).

For the biological pathway (BP) enrichment analysis (Fig. 3C,D), LSAfun and rrvgo packages in R were used to reduce GO BP terms by identifying redundancy based on semantic similarity. Treemaps representing parent GO BP terms were made using the treemapify package in R (Fig. 3C,D). GGPlot2 was used to plot the top 10 enriched parent terms associated with genes maximally bound at E11.5, E13.5, E15.5 and E17.5 were plotted.

For parent pathway enrichment analyses (Fig. S3, Fig. 5E), the complete list of pathways (Table S13a) was downloaded from the REACTOME database, along with a pathway hierarchy relationship file that contained columns with REACTOME parent pathway (top tier) and child pathway (second or third tier) identifiers (Table S13b). From the complete list of pathways (Table S13a), we then identified pathways associated only with mouse genes. Next, we used the REACTOME pathways enriched for dynamic, partially dynamic and stable genes to identify the corresponding parent pathways in R (Table S13b). This produced a list of parent pathways for each category (dynamic, partially dynamic, and stable). Enriched parent pathways were then plotted using GGPlot2 in R. A similar method was used for maximally bound genes at each timepoint (Fig. 3F) and DL-STAU2 cargo vs not cargo genes (Fig. 5E).

Comparisons with published datasets

Genes in STAU2 cargo were compared to pro-IPC (ON) and non-IPC (OFF) gene lists generated by Aprea et al., 2012 and overlapping genes were identified using the inner_join function (dplyr library) in R (Fig. 4C,D). Heatmaps showing the average

expression of these genes across the four time points were generated using the heatmap.2 function in R. Weighted mean expressions were calculated by applying peak scores as weights to read counts at each timepoint. This allowed us to quantify mean binding of STAU2 to cargo genes across the different captured regions. Weighted mean expressions of STAU2 cargo genes were used for this analysis.

Similarly, VZ, SVZ, and CP gene lists were obtained from the Fietz et al., 2013 study. STAU2 cargo genes were compared to these gene lists as described above and lists of overlapping genes were (GZ-Cargo) obtained. Markers present in genelists but not present in STAU2 cargo were designated GZ-Not Cargo. To obtain the DNA-binding (DB) genes, these overlapping genes were further filtered based on the 'transcription DNA-templated' term (GO:0006351) in the Gene Ontology (GO) database using the 'get_anno_genes' function (GofuncR library) in R. Heatmaps representing this data were generated as described above (Fig. 5A, S5B). Weighted mean expressions of STAU2 cargo genes were used for this analysis.

For phenotypic enrichment analysis, the DB gene lists obtained above were analyzed using the Mouse Genome Informatics (MGI) database (http://www.informatics.jax.org/batch) (Bult et al. 2019), and Mammalian Phenotype Ontology Enrichment (Smith & Eppig 2009) was determined through the MouseMine portal (Motenko et al. 2015). Graphs based on this data were generated in R (Fig. 5B,C).

For layer marker analysis, calibrated probabilities of genes enriched in cortical layers II-III, layer IV, layer V, layer VI and layer VIb were obtained from Belgard et al. 2011. Mean probabilities for layers II/III/IV (upper layer (UL)) and V/VI/VIb (deep layer (DL)) were determined. Probability values were scaled using the empirical cumulative distribution function (ECDF) function in R. Genes with mean scaled probabilities >0.9 were selected. Unique genes in each group were categorized as UL or DL markers. The cumulative expression of STAU2-bound layer markers was analyzed using a weighted means approach. Weights, ie. scaled probabilities of genes being specific for UL or DL, were used to calculate the weighted mean expression of UL and DL markers in the

cargo at the four timepoints. A line graph with a 90% confidence interval was generated showing the mean layer marker expression in STAU2 cargo (Fig. 5D).

Analysis of endothelial cell markers in the cargo

To assess whether there was significant post-lysis binding, we assessed STAU2 expression in a single cell dataset (Loo et al., 2019), and found that expression in endothelial cells (ECs) is much lower than other cell types at E14.5 in mouse. However, other studies indicate STAU2 is expressed in ECs in single cells derived from developing mouse brains and spinal cords (P2 and P11) (Rosenberg et al., 2018) and adult mouse brain ((Zhang et al., 2014)- https://www.brainrnaseq.org/, (Zeisel et al., 2015)- http://linnarssonlab.org/cortex/). Nevertheless, given the relatively low EC expression we rationalized that if there was extensive post-lysis binding this would be reflected in high EC transcript presence in the STAU2 cargo.

Using a database of mouse EC markers enriched over whole brain (Daneman et al., 2010), we evaluated the top 100 genes most highly enriched in ECs and found only 7 present in the cargo. Most common EC markers such as *Pecam1, Pglyrp1, Tie1, Epas1, Flt1 and Fli1* were absent from our dataset, and just two specific EC markers, *Tek* and *Kdr* were present. As STAU2 may be expressed at a low level in ECs, we cannot rule out the possibility that STAU2 is genuinely binding these RNAs in ECs. Taken together, these observations are consistent with negligible post-lysis binding captured in the dataset.

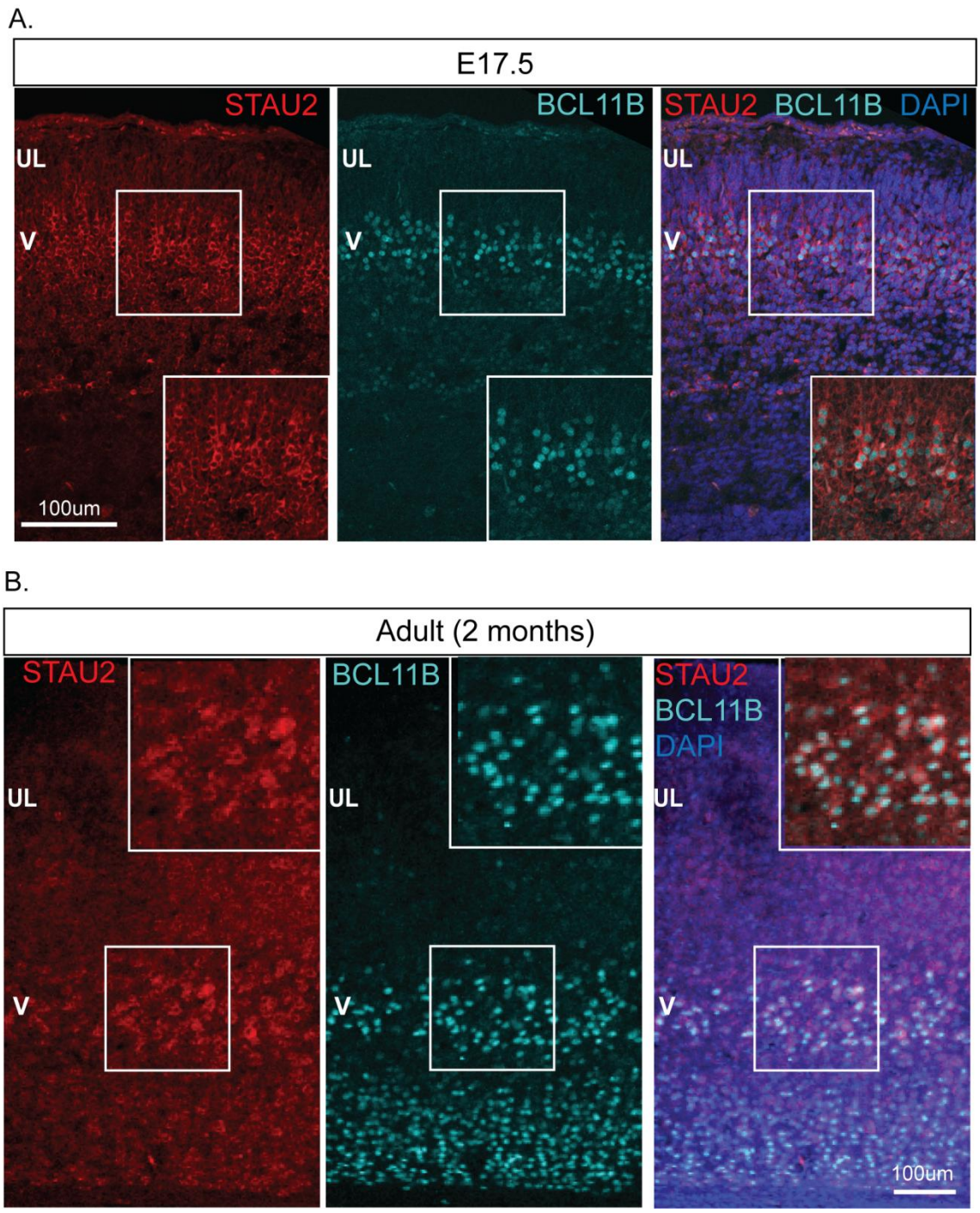

Fig. S1. (relates to Fig. 1). STAU2 is strongly expressed in BCL11B+ layer V cells in the developing and adult cortex. Immunohistochemistry using a STAU2-specific mouse monoclonal antibody in coronal sections revealed co-expression of STAU2 and BCL11B (CTIP2) at E17.5 (A) and 2 months (B). Scale bars= 100 μm.

A.

Peak Score	No. of peaks
<10	12763
10-100	18795
100-1000	3246
1000-10000	201
>10000	29

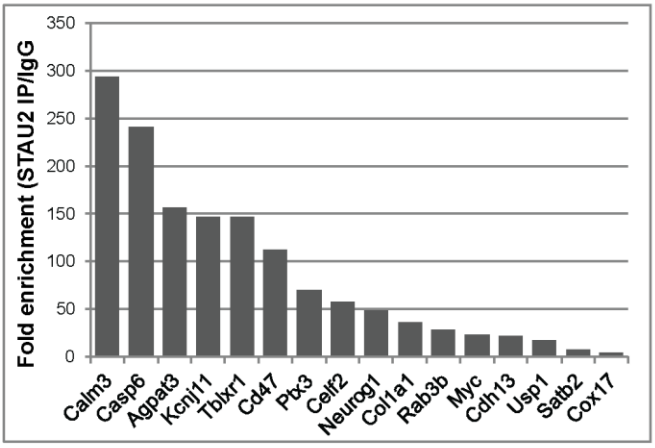

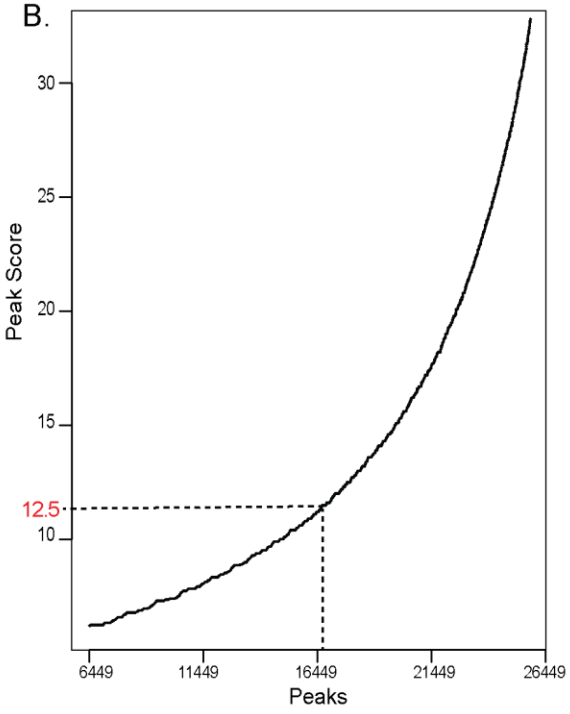

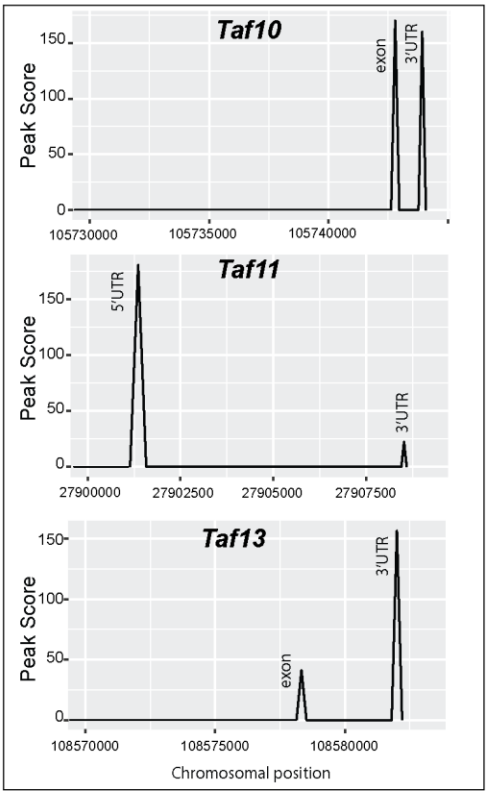

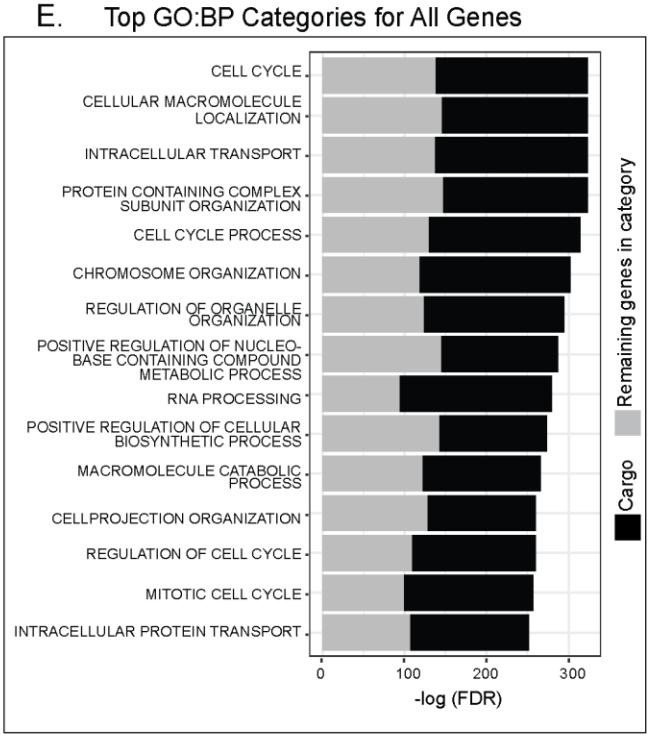

Fig. S2. (relates to Fig 2). (A) Table showing number of peaks in the STAU2 cargo for designated ranges of peak scores. (B) Line graph representing the distribution of peaks, where the X-axis represents peaks, and peak score is plotted on

the Y-axis. The elbow point (dotted lines) was determined to be 12.5 and this was set as peak score cut-off to determine the most enriched peaks. (C) qRT-PCR was used to validate presence of candidate genes in STAU2 RIPs over negative control IgG at E15.5. (D) Depiction of the transcript regions captured for representative genes, *Taf10, Taf11 and Taf13*. Peaks observed corresponded to exon and 3'UTR for *Taf10*, 5'UTR and 3'UTR for *Taf11*, and exon and 3'UTR for *Taf13*. (E) The top 15 GO BP categories associated with all transcripts in STAU2 cargo. To illustrate the contribution of STAU2 cargo to each category, the bars are filled to show the proportion of STAU2 cargo (black) versus the remaining genes in the category (grey).

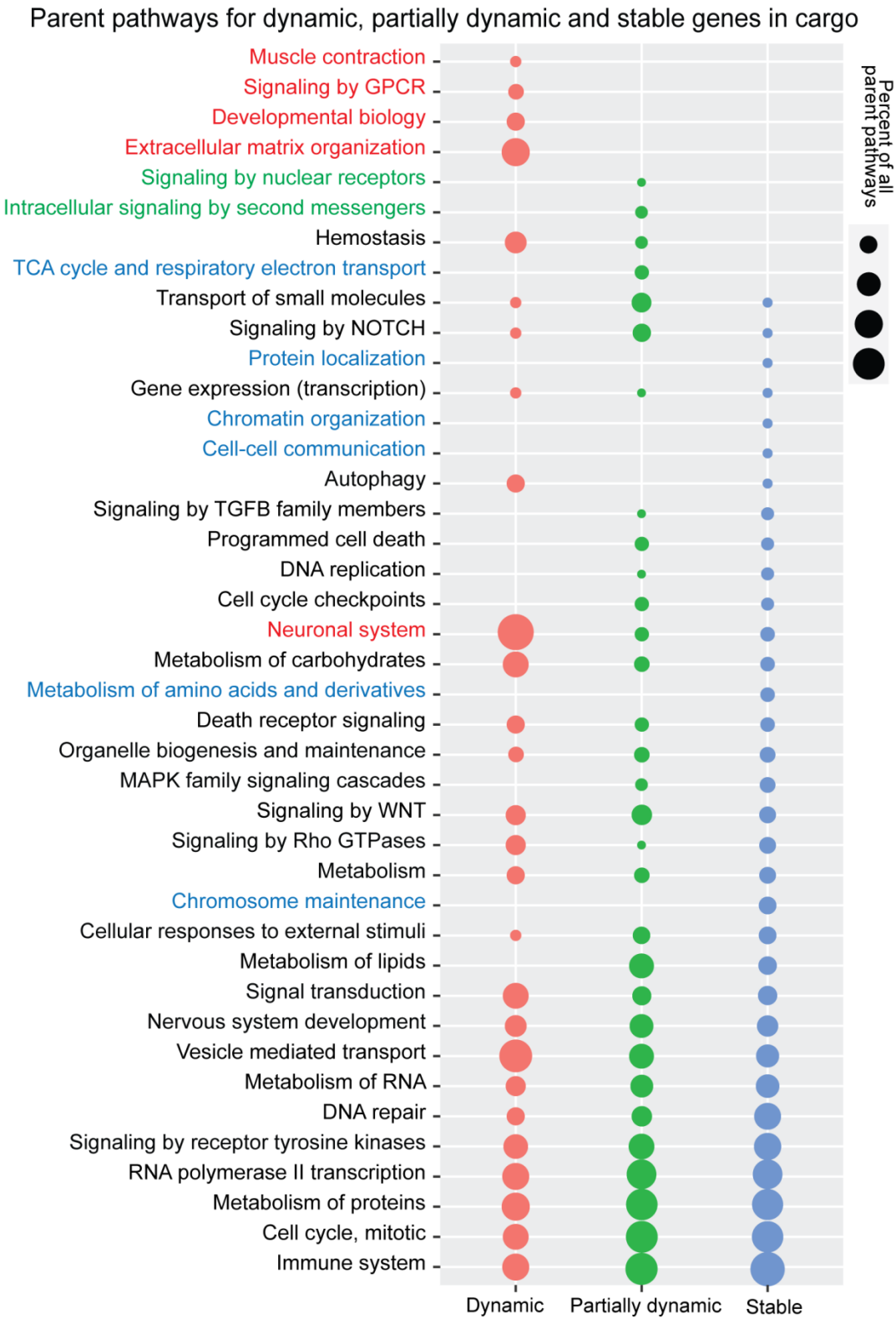

Fig. S3. (relates to Fig. 3). Balloon plot showing enriched REACTOME parent, ie. the top tier and the second-tier pathways associated with dynamic, partially dynamic and stable genes in STAU2 cargo. Color in the legend refers to the stability and percent is indicated by dot size. Percent refers to the contribution of the specified category to all the enriched categories for that particular stability group. Parent pathways corresponding to at least one percent of all enriched pathways are shown. Parent pathways higher in the dynamic group are indicated in red text, those enriched in the partially dynamic group are highlighted in green text, and those higher in the stable group are in blue text.

A.

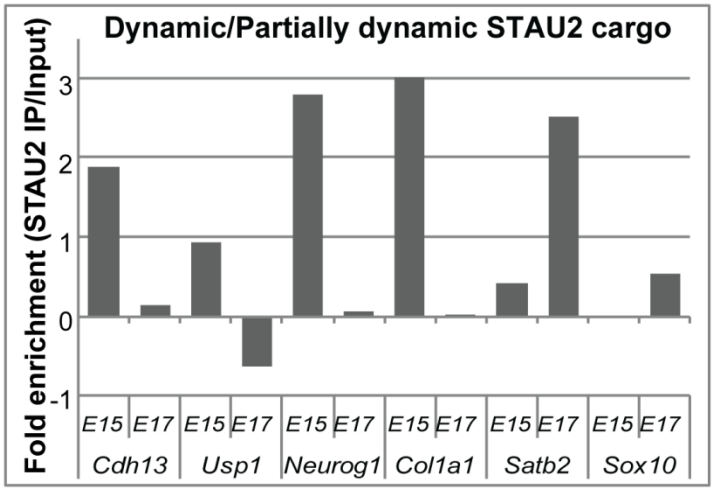

B.

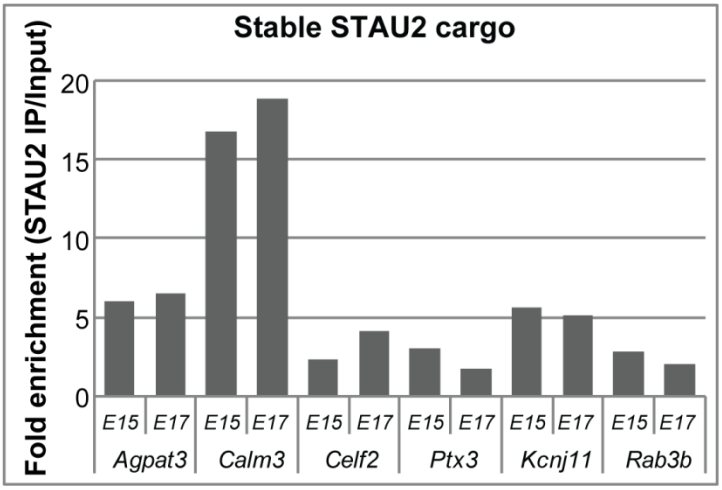

Fig. S4. (relates to Fig. 4). (A) qRT-PCR was used to validate presence of candidate genes in STAU2 RIPs over negative control IgG at E15.5. (B, C) Validation of dynamic and partially dynamic STAU2 cargo genes, *Cdh13*, *Usp1*, *Neurog1*, *Col1a1 and Satb2 and stable STAU2 cargo genes, Agpat3, Calm3, Celf2, Ptx3, Kcnj11 and Rab3b in RNA isolated from STAU2 RIPs using E15.5 and E17.5 mouse cortical tissue. Y-axis represents fold enrichment in STAU2 IP over input.*

A.

	VZ	SVZ	VZ/SVZ	CP
Total (Fietz et al.)	2234	394	783	1543
Genes in cargo	1055	184	389	768
DB genes in cargo	242	44	101	91
DB genes in cargo-Dynamic	137	32	57	67
DB genes in cargo-Stable	106	12	44	24
DB genes not in cargo	142	31	54	74

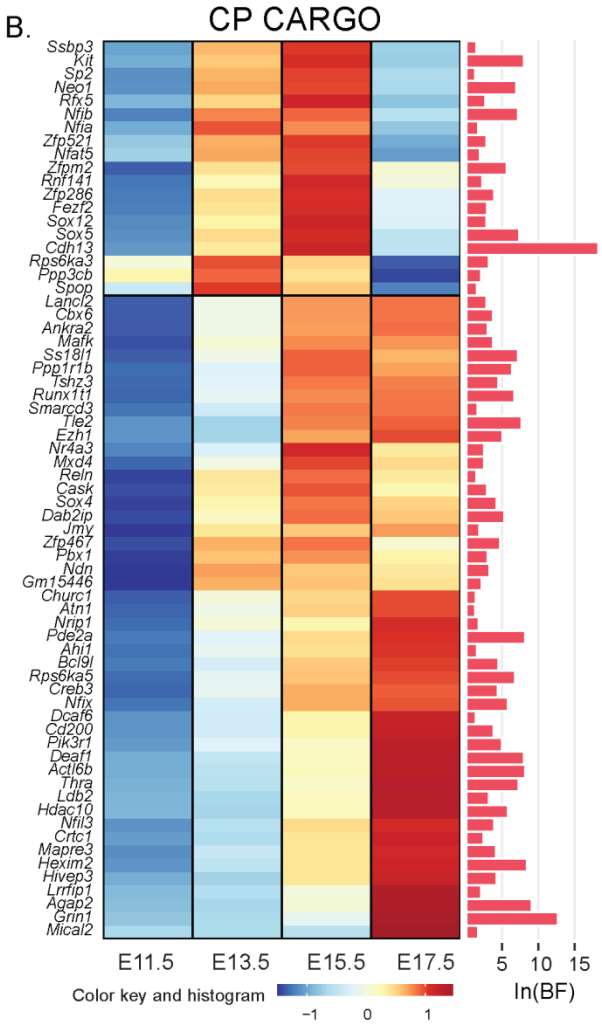

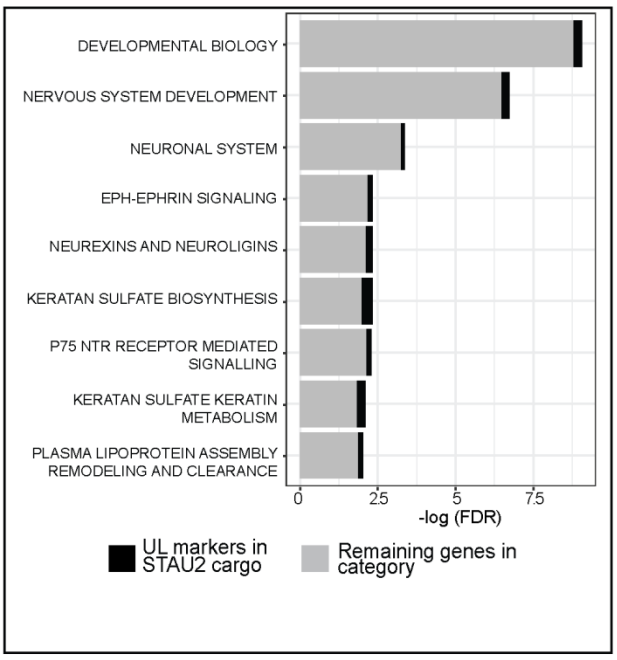

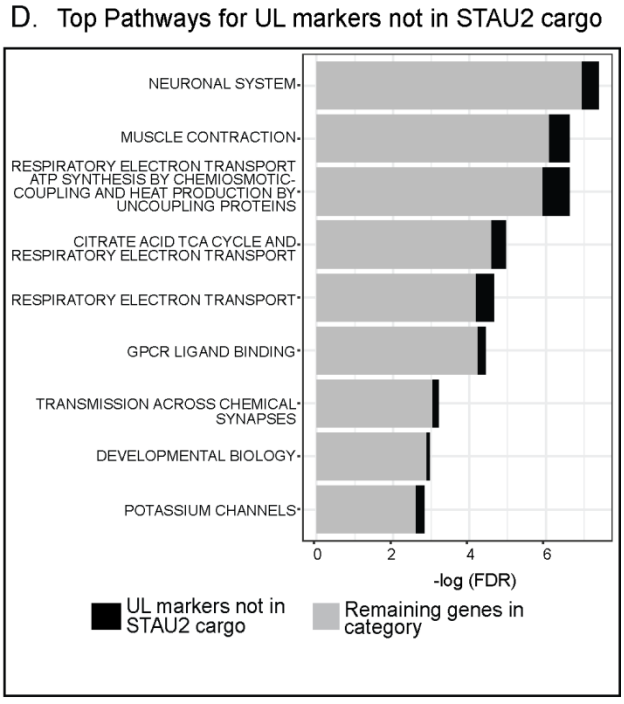

Fig. S5. (relates to Fig. 5). Comparison of STAU2 cargo with published datasets. Quantification of VZ, SVZ, VZ-SVZ and CP genes identified by Fietz et al., 2012, those present in the cargo, and DNA-binding genes in cargo and not in cargo for each zone. (B) Heatmap showing the average expression of dynamic and partially dynamic

CP-DB genes in the STAU2 cargo from E11.5 to E17.5. The horizontal bar graph on the right of the heatmap represents ln(BF). Color key represents z-score after scaling across rows, with red signifying higher expression and purple signifying lower expression. (C) The top REACTOME pathways differentially enriched for UL transcripts in STAU2 cargo. (D) The top enriched REACTOME pathways for transcripts identified as UL markers that were not present in STAU2 cargo. To illustrate the contribution of STAU2 cargo to each category, the bars are filled to show the proportion of STAU2 cargo or not cargo genes (black) versus the remaining genes in the category (grey).

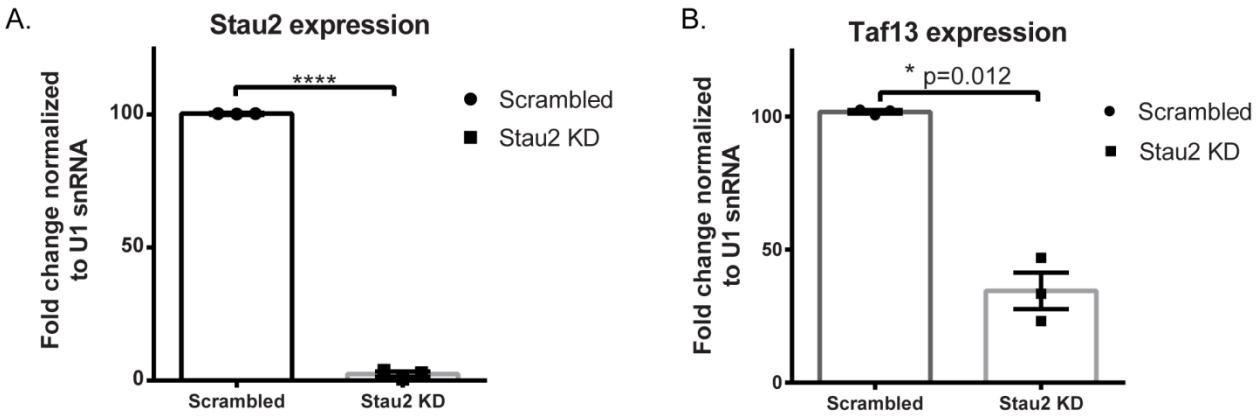

Fig. S6. (relates to Fig. 6). Knockdown of *Stau2* leads to a reduction in *Taf13* expression. E12.5 mouse cortices were dissected, dissociated, and infected with scrambled shRNA as control or shRNAs targeting *Stau2* at MOI=3, and cultured for 3 DIV. qRT-PCR was used to quantify the reduction of *Stau2* (A), and *Taf13* (B) expression. Fold change in expression was normalized to U1 snRNA. *p <0.05, paired student's t test, n=3. Graphs show means+/-SEM.

Table S1. STAU2 RIP-seq peaks file with count data

Click here to download Table S1

Table S2. Pairwise comparison of ln(BF)s assigned to STAU2 cargo genes at different time points and summed ln(BF).

Click here to download Table S2

Table S3. GO biological process (BP) and REACTOME pathway enrichment of all STAU2 cargo.

a) List of GO biological processes (BP) associated with all STAU2 cargo genes.
b) List of REACTOME pathways associated with all STAU2 cargo genes.

For all GO BP and pathways enrichment analyses, 'signature' refers to total genes analyzed, 'geneset' refers to the total number of genes associated with the category, and 'overlap' refers to the number of genes in the cargo that match the geneset.

Click here to download Table S3

Table S4. GO biological process (BP) and REACTOME pathway enrichment of dynamic STAU2 cargo.

a) List of GO biological processes (BP) associated with dynamic STAU2 cargo genes.
b) List of REACTOME pathways associated with dynamic STAU2 cargo genes.
c) Parent BP terms for dynamic STAU2 cargo genes (treemap data)

Click here to download Table S4

Table S5. GO biological process (BP) and REACTOME pathway enrichment of partially dynamic STAU2 cargo.

a) List of GO biological processes (BP) associated with partially dynamic STAU2 cargo genes.
b) List of REACTOME pathways associated with partially dynamic STAU2 cargo genes.
c) Parent BP terms for partially dynamic STAU2 cargo genes (treemap data)

Click here to download Table S5

Table S6. GO biological process (BP) and REACTOME pathway enrichment of stable STAU2 cargo.

a) List of GO biological processes (BP) associated with stable STAU2 cargo genes.
b) List of REACTOME pathways associated with stable STAU2 cargo genes.
c) Parent BP terms for stable STAU2 cargo genes (treemap data)

Click here to download Table S6

Table S7. REACTOME parent pathways associated with dynamic, partially dynamic and strongly stable STAU2 cargo.

a) List of REACTOME parent pathways associated with dynamic STAU2 cargo genes.
b) List of REACTOME parent pathways associated with partially dynamic STAU2 cargo genes.
c) List of REACTOME parent pathways associated with stable STAU2 cargo genes.
d) Table showing the percentage of contribution of a particular category to all enriched REACTOME parent categories for dynamic, partially dynamic and strongly stable STAU2 cargo pathways.

Click here to download Table S7

Table S8. Parent GO biological process (BP) enrichment of STAU2 cargo genes maximally bound at E11.5, E13.5, E15.5 and E17.5.

a) List of GO BO terms and parent terms associated with genes maximally bound at E11.5.
b) List of GO BO terms and parent terms associated with genes maximally bound at E12.5.
c) List of GO BO terms and parent terms associated with genes maximally bound at E13.5.
d) List of GO BO terms and parent terms associated with genes maximally bound at E17.5.
e) Table showing the percentage of contribution of a particular category to top 10 enriched parent categories for STAU2 cargo with highest binding at each time point.
f) Lists of genes with maximum binding at each time point.

Click here to download Table S8

Table S9. Pro-IPC and Non-IPC genes in cargo

a) Read counts and summed ln(BF)s of pro-IPC genes in STAU2 cargo.
b) Read counts and summed ln(BF)s of non-IPC genes in STAU2 cargo.

Click here to download Table S9

Table S10. Phenotypic enrichment of VZ-DB, SVZ-DB and CP-DB genes

a) Gene lists corresponding to VZ, SVZ, VZ-SVZ, CP DNA-binding (DB) genes in present cargo, stable and dynamic SVZ (SVZ+VZ-SVZ)-DB and VZ-DB genes in STAU2 cargo, and VZ, SVZ, VZ-SVZ, CP DB genes not in STAU2 cargo. Dynamic=dynamic and partially dynamic STAU2 cargo genes. Stable= stable and strongly stable STAU2 cargo genes.
b) Mammalian Phenotype (MP) terms enriched for VZ-DB cargo and not cargo genes downloaded from the MouseMine portal.
c) Mammalian Phenotype (MP) terms enriched for SVZ-DB cargo and not cargo genes downloaded from the MouseMine portal.
d) Mammalian Phenotype (MP) terms enriched for VZ-SVZ-DB cargo and not cargo genes downloaded from the MouseMine portal.
e) Mammalian Phenotype (MP) terms enriched for CP-DB cargo and not cargo genes downloaded from the MouseMine portal.
f) Mammalian Phenotype (MP) terms enriched for dynamic+partially dynamic and stable VZ-DB and SVZ(VZ+VZ-SVZ)-DB cargo downloaded from the MouseMine portal.

Click here to download Table S10

Table S11. REACTOME pathway enrichment of deep layer (DL) and upper layer (UL) markers in STAU2 cargo and those not present in STAU2 cargo.

a) List of REACTOME pathways associated with DL markers present in STAU2 cargo.
b) List of REACTOME pathways associated with DL markers not present in STAU2 cargo.
c) List of REACTOME parent pathways associated with DL markers present in STAU2 cargo.
d) List of REACTOME parent pathways associated with DL markers not present in STAU2 cargo.
e) Table showing the percentage of contribution of a particular category to all enriched REACTOME parent categories for DL STAU2 cargo and not cargo pathways.
f) List of REACTOME pathways associated with UL markers present in STAU2 cargo.
g) List of REACTOME pathways associated with UL markers not present in STAU2 cargo.
h) Lists of UL and DL markers present in STAU2 cargo and those not present in cargo.

Click here to download Table S11

Table S12. Primary antibody, primer and shRNA information.

Click here to download Table S12

Table S13. REACTOME complete list of pathways

a) A complete list of pathways downloaded from the REACTOME database.

b) Pathway hierarchy relationship file downloaded from the REACTOME database containing REACTOME parent pathway (top tier) and child pathway (second or third tier) identifiers.

Click here to download Table S13

References

Bult, C.J. et al., 2019. Mouse Genome Database (MGD) 2019. *Nucleic acids research*, 47(D1), pp.D801–D806.

Daneman, R., Zhou, L., Agalliu, D., Cahoy, J. D., Kaushal, A. and Barres, B. A. (2010). The Mouse Blood-Brain Barrier Transcriptome: A New Resource for Understanding the Development and Function of Brain Endothelial Cells. PLoS One 5, e13741.

Loo, L., Simon, J. M., Xing, L., McCoy, E. S., Niehaus, J. K., Guo, J., Anton, E. S. and Zylka, M. J. (2019). Single-cell transcriptomic analysis of mouse neocortical development. Nat. Commun. 10, 134.

Motenko, H. et al., 2015. MouseMine: a new data warehouse for MGI. *Mammalian genome : official journal of the International Mammalian Genome Society*, 26(7–8), pp.325–330.

Rosenberg, A. B., Roco, C. M., Muscat, R. A., Kuchina, A., Sample, P., Yao, Z., Graybuck, L. T., Peeler, D. J., Mukherjee, S., Chen, W., et al. (2018). Single-cell profiling of the developing mouse brain and spinal cord with split-pool barcoding. Science (80-.). 360, 176 LP-182.

Smith, C.L. & Eppig, J.T., 2009. The mammalian phenotype ontology: enabling robust annotation and comparative analysis. *Wiley interdisciplinary reviews. Systems biology and medicine*, 1(3), pp.390–399.

Zeisel, A., Muñoz-Manchado, A. B., Codeluppi, S., Lönnerberg, P., La Manno, G., Juréus, A., Marques, S., Munguba, H., He, L., Betsholtz, C., et al. (2015). Cell types in the mouse cortex and hippocampus revealed by single-cell RNA-seq. Science (80-.). 347, 1138 LP-1142.

Zhang, Y., Chen, K., Sloan, S. A., Bennett, M. L., Scholze, A. R., O'Keeffe, S., Phatnani, H. P., Guarnieri, P., Caneda, C., Ruderisch, N., et al. (2014). An RNA-Sequencing Transcriptome and Splicing Database of Glia, Neurons, and Vascular Cells of the Cerebral Cortex. J. Neurosci. 34, 11929 LP-11947.